Parametric Image Reconstruction for ECT-like Sensor with Applications in Two-Phase Flow

Hector Lise de Moura, Daniel Rodrigues Pipa, Aluisio do Nascimento Wrasse and Marco Jose Da Silva

***Abstract*— Electrical Capacitance Tomography (ECT) is a technique developed to estimate phase distribution in pipelines. Most ECT instruments, however, suffer from high peripheral / low central sensitivities. This ill conditioning causes the reconstruction to be unstable, producing low quality images.**

This paper presents a new method for an ECT inspired sensor that was developed in a previous work of our group. Although the sensor was designed with few electrodes for simplicity, this worsened general sensitivity, restricting the use of classical reconstruction methods. This paper addresses this issue by applying a parametric approach, improving overall quality of the reconstructed image.

***Keywords*— ECT, image reconstruction, parametric methods, alternate minimization, two-phase flow, stratified flow.**

I. Introduction

Two-phase flows are very common in many industrial sectors, especially in the petroleum industry. When gas and liquid stream simultaneously in a pipe, some patterns may develop depending on their individual velocities. Figure 1 illustrates the most common arrangements.

The knowledge of the distribution of each component, known as phases, is of great importance to the safety and efficiency of plants. Many instruments aiming at estimating those distributions have been developed: wire-mesh [1], optical tomography [2], high-speed videometry [3], ultrassound [4] are some examples, just to name a few.

Among them, Electrical Capacitance Tomography (ECT) has been played an important role. Since some fluids display different electrical permittivities, ECT is able to sense variations of this properties inside a pipe and, through appropriate reconstruction algorithms, can determine characteristics of the flow such as phase distribution.

In most ECT systems, N electrodes are circularly disposed around a vessel and instrument system the capacitance between every electrode pairs. Because the sensitive region of each electrode pair often overlap, a process referred to as *image reconstruction* must be performed to unscramble the data and generate a *image* of the permittivity distribution.

Image reconstruction on ECT is an ill-posed inverse problem because the desired image is often larger than the data acquired and the sensitivity to the permittivity close to the center axis of the pipe is low.

Hector Lise de Moura, Departament of Eletronic Engineering. Daniel Rodrigues Pipa, Aluisio do Nascimento Wrasse and Marco Jose da Silva, Graduate Program in Electrical and Computer Engineering.Federal University of Technology - Paraná, Brazil. E-mails: hector@alunos.utfpr.edu.br, danielpipa@utfpr.edu.br, aluisionw@yahoo.com.br, m.dasilva@ieee.org.

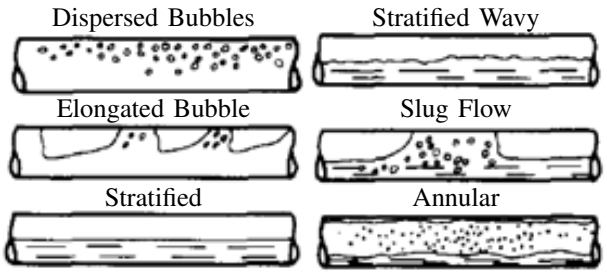

Fig. 1. Common patterns of gas-liquid two-phase flows. This work is manly concerced with Stratified or Stratified Wavy patterns. Source: [11]

Many methods have been proposed to solve this inverse problem, such as Linear Back Projection [5], Landweber Iteration [6] and Tikhonov regularization [7]. More recently, methods that use the sparsity-promoting l_1-norm have produced promising result [8]–[10]. Usually, the l_1-norm is combined with a finite difference operator giving rise to the so-called Total Variation (TV) regularization. Unlike other penalty functions that result in oversmoothed images, TV allows abrupt transitions and the resulting images tend to look shaper.

Parametric reconstruction algorithms have been proposed for ECT. In [12], the authors adopt an ellipsoid parametric description of the permittivity distribution and use a Levenberg-Marquardt algorithm to estimate its parameters. In [13], the authors also use an ellipse to describe the distribution, but employ Monte Carlo techniques to solve the optimization problem.

Similarly, this paper proposes a parametric image reconstruction algorithm for an ECT-inspired sensor developed in our group [14]. Due to the reduced number of electrodes (only 8), nonparametric reconstruction algorithms either results in a low resolution image, or become highly unstable as the number of unknowns outdistance the number of data points.

II. Sensor Design

The sensor considered in this work is composed by eight receiving electrodes and a transmitter ring electrode. It consists of a thin copper sheet, applied over a low-cost Kapton tape, and etched in order to form the electrodes. Figure 2 shows a picture of the prototype mounted on the inner wall of a pipe. Figure 3 shows a model of the sensor designed in COMSOL.

A Direct Digital Synthesizer (DDS) generates sine waves that are applied to the transmitter electrode. The signals from the eight electrodes are conditioned by transimpedance amplifiers and sampled by a signal acquisition card. The

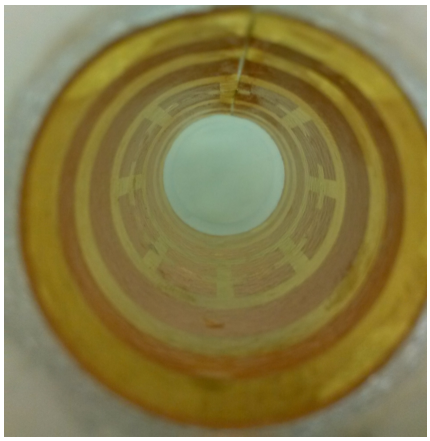

Fig. 2. Prototype sensor mounted on the inner wall of a pipe. The sensor is composed by eight eletrodes distributed around the perimeter. Source: [14].

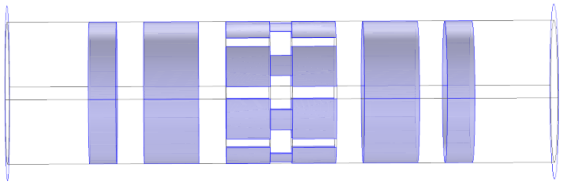

Fig. 3. Sensor model. Receiver electrodes in the middle, guard rings on the far sides and transmitter electrodes in between.

voltage measurements are proportional to the capacitance at each electrode pair and are given by [15]

$$V_o = -V_i \frac{C_x}{C_f},$$

where V_i is the amplitude of the sine waves, C_x is the unknown capacitance and C_f is the capacitor present in the transimpedance amplifier. As V_i and C_f are constants, it is possible to obtain the values of C_x after a calibration routine.

III. Reconstruction Algorithm

Although the ECT is a fundamentally a nonlinear problem, we follow most reported works [16] and adopt a linearized model given by

$$\mathbf{g} = \mathbf{S}\mathbf{f} + \mathbf{n},$$

where $\mathbf{g}$ is a vector representing the capacitance measurements, $\mathbf{S}$ is the sensitivity matrix, $\mathbf{f}$ is a vector of the permittivity distribution and $\mathbf{n}$ is the measurement noise vector. The sensitivity matrix linearizes the problem around some reference point $\mathbf{f}_0$.

A more accurate, finite element model of the sensor was built in COMSOL. The model permits nonlinear simulations of capacitance measurements from predefined permittivity distributions. Based on an average permittivity and the procedure described in [17], we simulated capacitance readings and calculated each element of $\mathbf{S}$ by

$$s_{ik} = \mu_i \times \frac{g_k(f_i + \delta f) - g_k(f_i)}{\delta f},$$

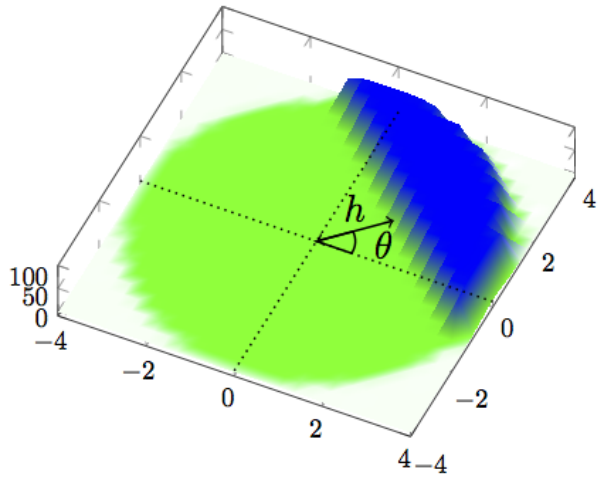

Fig. 4. Hyperbolic tangent surface proposed as continuous differentiable surface to model permissivity distribuition for a stratified flow. Here, $h = 2.5$ and $\theta = \pi/4$.

where μ_i denotes the volume normalization factor of the i-th in-pipe element, g_k is the capacitance measured at the k-th electrode, f_i is the electric permittivity at the i-th in-pipe element and δf is the perturbation applied.

Most ECT reconstruction algorithms attempt to estimate $\mathbf{f}$ using a minimization strategy, e.g.

$$\mathbf{f} = \arg\min_{\mathbf{f}} \frac{1}{2} \|\mathbf{g} - \mathbf{S}\mathbf{f}\|^2 + \lambda \Psi(\mathbf{f}), \qquad (1)$$

where $\Psi(\cdot)$ is some penalty function, often to reinforce smoothness and improve stability, and λ is the regularization parameter. A well-known penalty is the TV, given by

$$\Psi_{\text{TV}}(\mathbf{f}) = \|\mathbf{D}\mathbf{f}\|_1,$$

where $\mathbf{D}$ is a vertical and horizontal finite difference matrix.

However, as the number of measurements is reduced and the measurement matrix is ill-conditioned, solving (1) is quite unstable. Although regularization stabilizes the solution, the problem is still highly underdetermined. For instance, to reconstruct a 16×16-pixel image, we need to estimate 256 variables from 8 data points.

Rather than using a nonparametric strategy, we propose to parametrize the permittivity distribution for stratified flow based on a hyperbolic tangent surface with two parameters: height (h) and angle (θ). The vector representing the permittivity distribution is, then, given by

$$\mathbf{f}(\theta, h) = \tanh\left[\mathbf{x}\sin(\theta) + \mathbf{y}\cos(\theta) - h\right] a + b, \qquad (2)$$

where the vectors $\mathbf{x}$ and $\mathbf{y}$ form the coordinate pairs for each pixel in the image, h is the offset of the image edge, θ is the angle of the phase transition and a and b are related to the minimum and maximum permittivity allowed by the instrument.

Figure 4 exemplifies a parametrized image of the flow. The blue region represents the liquid ($\epsilon_r = 80$ for water) and the green region represents the gas ($\epsilon_r = 1$ for air).

Since the proposed parametrization is a continuous differentiable function, we can resort to simple gradient-based

optimization procedures. Assuming Gaussian noise, a simple Maximum Likelihood (ML) strategy is

$$\hat{h}, \hat{\theta} = \arg\min_{h,\theta} \frac{1}{2} \|\mathbf{g} - \mathbf{S}\mathbf{f}(h, \theta)\|^2 . \quad (3)$$

To solve (3), we use Gradient Descent iterations

$$\mathbf{n}_{k+1} = \mathbf{n}_k - \eta \nabla \mathbf{f}(\mathbf{n}_k) \quad (4)$$

performing an alternate minimization for both parameters.

Expanding (4) for θ and h, we obtain

$$\theta_{k+1} = \theta_k - \eta_1 \left(\frac{\partial \mathbf{f}(\theta_k, h_k)}{\partial \theta_k} \right)^{\mathrm{T}} \mathbf{S}^{\mathrm{T}}(\mathbf{g} - \mathbf{S}\mathbf{f}(\theta_k, h_k)) \quad (5)$$

$$h_{k+1} = h_k - \eta_2 \left(\frac{\partial \mathbf{f}(\theta_k, h_k)}{\partial h_k} \right)^{\mathrm{T}} \mathbf{S}^{\mathrm{T}}(\mathbf{g} - \mathbf{S}\mathbf{f}(\theta_k, h_k)) \quad (6)$$

The partial derivatives in (5) and (6) are respectively:

$$\frac{\partial \mathbf{f}(\theta_k, h_k)}{\partial \theta_k} = \operatorname{sech}^2(\mathbf{v}(\theta_k, h_k)) \circ (\mathbf{x}\cos(\theta_k) - \mathbf{y}\sin(\theta_k))\, a$$

and

$$\frac{\partial \mathbf{f}(\theta_k, h_k)}{\partial h_k} = \operatorname{sech}^2(\mathbf{v}(\theta_k, h_k))a,$$

where

$$\mathbf{v}(\theta, h) = \mathbf{x}\sin(\theta) + \mathbf{y}\cos(\theta) - h\mathbf{1}.$$

Here, $\circ$ stands for Hadamard or element-wise product and $\mathbf{1}$ is a vector composed by ones.

Finally, the algorithm can be summarized in the following steps:

(a) Initialize η_1, η_2, $\mathbf{f}_0 = \mathbf{S}^{\mathrm{T}}\mathbf{g}$, $h = 0$ and $\theta = 0$.
(b) For $k = 1$ to some maximum number of iterations, do:
   1. Update θ_{k+1} using (5), while keeping h unchanged.
   2. Update h_{k+1} using (6), while keeping θ unchanged.
   3. Update $\mathbf{f}_{k+1} = \mathbf{f}(h_{k+1}, \theta_{k+1})$ using (2).
   4. Repeat until some stop criterion.

IV. Results

We simulated in COMSOL capacitance readings for an air-water stratified flow using several values of h and θ. We reconstructed permittivity images using the a Total Variation approach [18], a Modified TV described in [10] and the proposed method.

Noise to 50dB of SNR was added to the data vector. The step sizes were experimentally chosen as $\eta_1 = 1 \times 10^{22}$ and $\eta_2 = 3 \times 10^{23}$. For the TV and Modified TV, we used the parameters suggested by the authors in their papers [8], [10].

Figures 5 through 7 show visual comparisons between the three methods. All the images, except for the proposed method, were interpolated by a factor of 10 using cubic splines to improve visualization.

Figure 5 illustrates an angled stratified flow ($h = 0$, $\theta = 315°$). Figure 5(b) shows the results for the anisotropic TV with the typical accentuation of horizontal and vertical edges. Figure 5(c) shows the results for the Modified TV proposed in [10]. The improvement over TV is attributed to the addition of matrix to compensate for the nonlinearities. Figure 5(d) illustrate the results of the proposed algorithm. Since it is parametric, we are able to generate the visualization at any desired resolution.

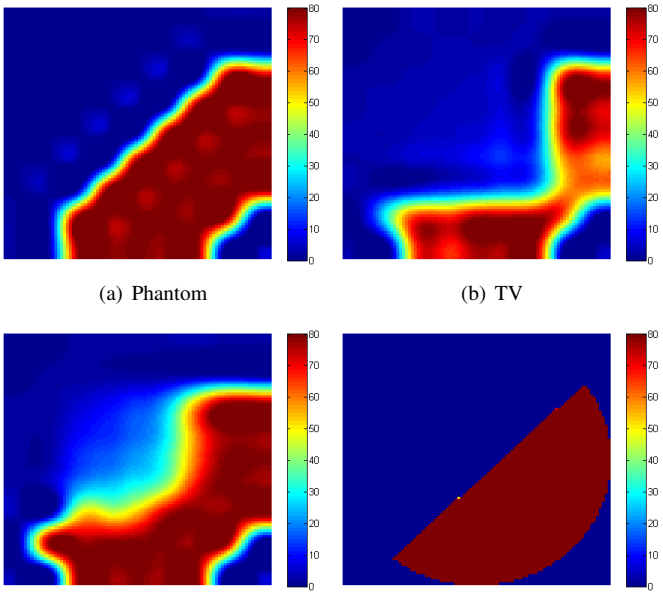

(a) Phantom (b) TV

(c) Modified TV (d) Proposed Algorithm

Fig. 5. Visual comparison between the three methods for an angled stratified flow ($h = 1$, $\theta = 315°$). Since the proposed method is parametric, we are able to generate the visualization at any desired resolution.

TABLE I
Mean Squared Error (MSE) for TV based algorithm. Average: 343, for $\lambda = 5.10^{-28}$.

$h\backslash\theta$	0°	45°	90°	135°	180°	225°	270°	315°
-3	320	213	318	206	322	218	321	283
-2	191	311	183	309	174	275	211	354
-1	412	403	363	400	375	482	481	450
0	39	431	63	452	29	567	107	479
1	38	581	6	648	311	659	53	668
2	324	565	297	578	491	673	315	603
3	106	508	74	506	146	594	90	561
4	243	456	275	457	227	505	235	445

Figure 6 presents similar results. A notable difference is that, as the image contains no diagonal edges, classical TV provided competitive results. Figure 7 show results for a slightly curved stratified flow. As our model does not support this feature, a deviation was expected.

Tables I, II and III summarize a battery of tests performed for different combinations of h and θ for all algorithms under evaluation. Despite local differences, classical TV provided an average mean square error of 343, against 261 of Modified TV and 202 of the proposed method.

V. Conclusion

This paper proposed a parametric ECT image reconstruction algorithm with applications to two-phase flow. When only a small number of measurements are available, parametric methods provide simple and stable reconstructions.

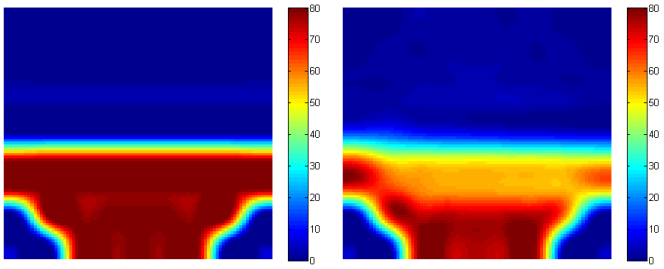

(a) Phantom (b) TV

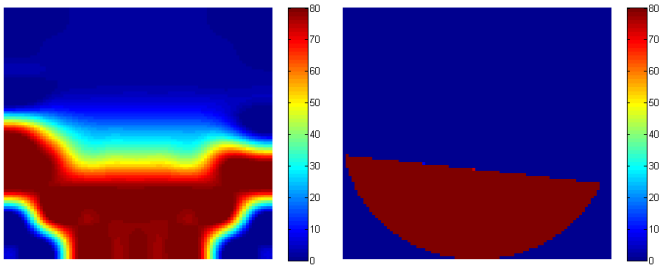

(c) Modified TV (d) Proposed Algorithm

Fig. 6. Comparison between the three methods for a horizontal stratified flow ($h = 1$, $\theta = 270°$).

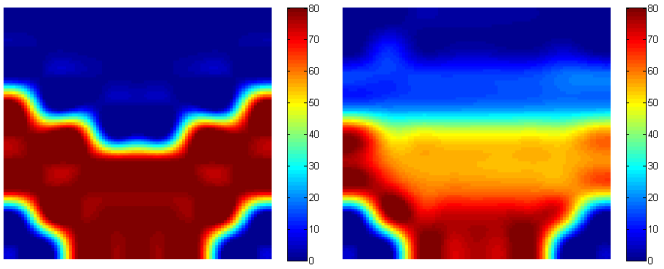

(a) Phantom (b) TV

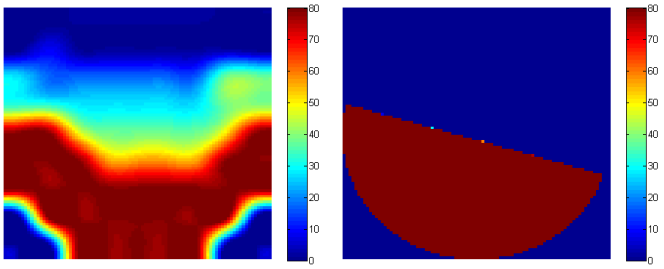

(c) Modified TV (d) Proposed Algorithm

Fig. 7. Comparison between the three methods for a slightly curved stratified flow ($h = 0$, $\theta = 270°$).

TABLE II

MSE FOR MODIFIED TV ALGORITHM. AVERAGE: 261, FOR $\lambda = 1.10^{-28}$.

$h\backslash\theta$	0°	45°	90°	135°	180°	225°	270°	315°
-3	368	152	369	163	365	147	366	205
-2	72	327	69	341	70	283	92	288
-1	367	290	274	273	283	332	250	242
0	318	460	337	376	258	410	233	352
1	69	391	70	225	97	238	63	216
2	451	433	488	344	495	291	449	349
3	76	342	136	309	108	343	77	334
4	255	129	273	188	205	126	258	126

TABLE III

MSE FOR PROPOSED ALGORITHM. AVERAGE: 202, FOR $\eta_1 = 1.10^{22}$ AND $\eta_2 = 3.10^{23}$.

$h\backslash\theta$	0°	45°	90°	135°	180°	225°	270°	315°
-3	645	291	62	281	50	292	61	287
-2	271	232	265	209	264	254	291	304
-1	188	186	194	187	185	223	394	263
0	89	70	81	72	80	89	293	77
1	80	110	43	111	103	210	427	115
2	85	63	85	63	76	157	83	63
3	48	63	45	65	45	162	51	63
4	31	54	58	60	47	93	31	59

We proposed a hyperbolic tangent surface as a parametric model for the permittivity distribution of stratified flow, which can represent the phase transition at any angle and any height. Moreover, since it is continuous and differentiable, we were able to use simple gradient-based to estimate the parameters.

The comparisons presented confirms the potential of the proposed method against state-of-the-art ECT algorithms. Future works include the extension of parametric model to use sparse representations of section being reconstructed.

VI. ACKNOWLEDGEMENTS

The authors acknowledge the financial support from following Brazilian Agencies: National Agency of Petroleum, Natural Gas and Biofuels (ANP), Financier of Studies and Projects (FINEP), Ministry of Science and Technology (MCT) and PETROBRAS, through the Human Resources Program of ANP for the Oil and Gas Sector - PRH- ANP/MCT.

REFERENCES

[1] M. Da Silva, S. Thiele, L. Abdulkareem, B. Azzopardi, and U. Hampel, "High-resolution gas-oil two-phase flow visualization with a capacitance wire-mesh sensor," *Flow Meas. Instrum.*, vol. 21, no. 3, pp. 191–197, Sep. 2010.

[2] T. P. Vendruscolo, M. V. W. Zibetti, R. L. Patyk, G. Dutra, R. E. M. Morales, C. Martelli, and M. J. Da Silva, "Development of NIR optical tomography system for the investigation of two-phase flows," in *Conf. Rec. - IEEE Instrum. Meas. Technol. Conf.*, 2014, pp. 1576–1579.

[3] C. E. F. do Amaral, R. F. Alves, M. J. da Silva, L. V. R. de Arruda, L. E. B. Dorini, R. E. M. Morales, and D. R. Pipa, "Image processing techniques for high-speed videometry in horizontal two-phase slug flows," *Flow Meas. Instrum.*, vol. 33, pp. 257–264, Oct. 2013.

[4] Y. Murai, Y. Tasaka, Y. Nambu, Y. Takeda, and S. R. Gonzalez A, "Ultrasonic detection of moving interfaces in gas–liquid two-phase flow," *Flow Meas. Instrum.*, vol. 21, no. 3, pp. 356–366, 2010.

[5] W. Q. Yang and L. Peng, "Image reconstruction algorithms for electrical capacitance tomography," *Meas. Sci. Technol.*, vol. 14, pp. R1–R13, 2002.

[6] W. Q. Yang, D. M. Spink, T. a. York, and H. McCann, "An image-reconstruction algorithm based on Landweber's iteration method for electrical-capacitance tomography," *Meas. Sci. Technol.*, vol. 10, pp. 1065–1069, 1999.

[7] L. Peng, H. Merkus, and B. Scarlett, "Using Regularization Methods for Image Reconstruction of Electrical Capacitance Tomography," *Part. Part. Syst. Charact.*, vol. 17, pp. 96–104, 2000.

[8] T. C. Chandrasekera, Y. Li, J. S. Dennis, and D. J. Holland, "Total variation image reconstruction for electrical capacitance tomography,"

in *2012 IEEE Int. Conf. Imaging Syst. Tech. Proc.*, vol. 50. IEEE, Jul. 2012, pp. 584–589.

[9] X. Wu, G. Huang, J. Wang, and C. Xu, "Image reconstruction method of electrical capacitance tomography based on compressed sensing principle," *Meas. Sci. Technol.*, vol. 24, no. 7, p. 075401, Jul. 2013.

[10] Y. Yang and L. Peng, "Data Pattern With ECT Sensor and Its Impact on Image Reconstruction," *IEEE Sens. J.*, vol. 13, no. 5, pp. 1582–1593, May 2013.

[11] J. M. Mandhane, G. a. Gregory, and K. Aziz, "A flow pattern map for gas-liquid flow in horizontal pipes," *Int. J. Multiph. Flow*, vol. 1, pp. 537–553, 1974.

[12] Y. Wang, L. Wu, M. Jia, L. Liu, H. Zhao, and F. Gao, "The Ellipsoid Parametric Description for the Shape-Based Image Reconstruction Algorithm of Diffuse Optical Tomography," in *Proc. SPIE Vol. 8578*, vol. 8578, 2013, pp. 1–9.

[13] K. Grudzien, A. Romanowski, R. G. Aykroyd, R. a. Williams, and V. Mosorov, "Parametric modelling algorithms in electrical capacitance tomography for multiphase flow monitoring," *Perspect. Technol. Methods MEMS Des. - Proceeding 2nd Int. Conf. Young Sci. MEMSTECH 2006*, no. 1, pp. 100–106, 2007.

[14] A. d. N. Wrasse, T. P. Vendruscolo, F. C. Castaldo, and M. J. da Silva, "Capacitive Array Sensor for Direct Imaging of Two-Phase Flows," in *15th Brazilian Congr. Therm. Sci. Eng.*, no. 1, Belém, Brazil, 2014, pp. 13–16.

[15] M. J. da Silva, E. Schleicher, and U. Hampel, "Capacitance wire-mesh sensor for fast measurement of phase fraction distributions," *Meas. Sci. Technol.*, vol. 18, pp. 2245–2251, 2007.

[16] D. Watzenig and C. Fox, "A review of statistical modelling and inference for electrical capacitance tomography," *Meas. Sci. Technol.*, vol. 20, p. 052002, 2009.

[17] C. G. Xie, S. M. Huang, B. S. Hoyle, R. Thorn, C. Lenn, D. Snowden, and M. S. Beck, "Electrical Capacitance Tomography for Flow Imaging - System Model for Development of Image-Reconstruction Algorithms and Design of Primary Sensors," *IEE Proceedings-G Circuits Devices Syst.*, vol. 139, no. 1, pp. 89–98, 1992.

[18] M. Soleimani and W. R. B. Lionheart, "Nonlinear image reconstruction for electrical capacitance tomography using experimental data," *Meas. Sci. Technol.*, vol. 16, no. 10, pp. 1987–1996, Oct. 2005.